

# DeepVigor+: Scalable and Accurate Semi-Analytical Fault Resilience Analysis for Deep Neural Networks

Mohammad Hasan Ahmadilivani<sup>1</sup>, Jaan Raik<sup>1</sup>, Masoud Daneshtalab<sup>1,2</sup>, Maksim Jenihhin<sup>1</sup>

<sup>1</sup>Tallinn University of Technology, Tallinn, Estonia

<sup>2</sup>Mälardalen University, Västerås, Sweden

Growing exploitation of Machine Learning (ML) in safety-critical applications necessitates rigorous safety analysis. Hardware reliability assessment is a major concern with respect to measuring the level of safety. Quantifying the reliability of emerging ML models, including Deep Neural Networks (DNNs), is highly complex due to their enormous size in terms of the number of parameters and computations. Conventionally, Fault Injection (FI) is applied to perform a reliability measurement. However, performing FI on modern-day DNNs is prohibitively time-consuming if an acceptable confidence level is to be achieved. In order to speed up FI for large DNNs, statistical FI has been proposed. However, the run-time for the large DNN models is still considerably long.

In this work, we introduce DeepVigor+, a scalable, fast and accurate semi-analytical method as an efficient alternative for reliability measurement in DNNs. DeepVigor+ implements a fault propagation analysis model and attempts to acquire Vulnerability Factors (VFs) as reliability metrics in an optimal way. The results indicate that DeepVigor+ obtains VFs for DNN models with an error less than 1% and 14.9 up to 26.9 times fewer simulations than the best-known state-of-the-art statistical FI enabling an accurate reliability analysis for emerging DNNs within a few minutes.

## I. INTRODUCTION

In recent years, the rapid advancement of Artificial Intelligence (AI), in particular of Machine Learning (ML), has provided a unique opportunity for automation leading to AI exploitation in safety-critical applications [1], [2]. Deep Neural Networks (DNNs) are dominantly employed in ML for complex tasks such as image classification and object detection that have applications in the safety-critical domain [3], [4]. According to recent regulations such as the European Union’s AI ACT [5] and the US National AI Initiative Act [6], AI systems that may cause adverse impacts on people’s safety are considered high-risk and must be rigorously assessed before deployment. This reflects the importance of early-stage safety risk assessment for AI deployment.

One of the major concerns in safety-critical applications is the hardware reliability of systems, which are threatened by hardware faults and errors [7]. With the technology miniaturization, the rate at which hardware faults occur is continuously rising in logic and memory circuits since the sensitivity of transistors increases against soft errors, temperature variations, etc. [8], [9], [10]. As DNNs are penetrating such applications e.g., perception in automotive [11], their hardware reliability assessment is necessary during the design and development phase, not only for risk certification but also for eliminating reliability weaknesses as early as possible.

On the other hand, the size of DNNs, in particular Convolutional Neural Networks (CNNs), in terms of memory footprint and number of operations is rapidly growing [12], [13]. Fig. 1 presents the growing model size in terms of the number of MAC operations and parameters for emerging DNNs and Vision Transformers (ViT), leading to their higher accuracy [14]. This trend necessitates leveraging more complex and performant computing systems such as GPUs, TPUs, etc. [15]. The fact that these complex systems are prone to hardware faults [16], [17], [18] leads to a necessary and complex task of their hardware reliability assessment prior to deployment in

safety-critical applications.

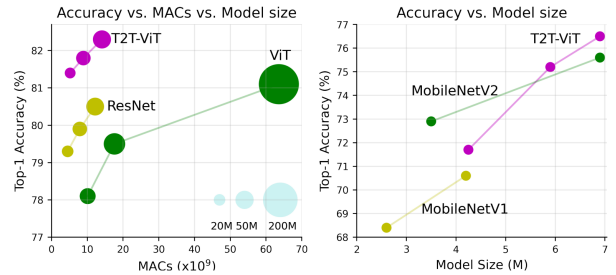


Fig. 1: Growing size of emerging DNN models regarding computation and memory requirement [14].

Hardware faults result in the alteration of values at the application level and might lead to erroneous outputs in a digital system. Hardware faults could lead to catastrophic consequences when exploiting hardware DNN accelerators in safety-critical applications. As an example, a hardware fault may result in misclassifying a red traffic light at an intersection in an autonomous vehicle and jeopardize the life of its passengers, as shown in Fig. 2, generated by AI.



Fig. 2: An example of hardware faults effect on an autonomous vehicle, generated by <https://getimg.ai>.

In this regard, several research works have been carried out to assess and enhance DNNs' hardware reliability against hardware faults listed in the related surveys [19], [16], [20], [21], [22]. Hardware reliability of DNN accelerators is the likelihood of a DNN accelerator performing as it is trained during the deployment [23]. The source of reliability threats is hardware-originated (soft errors, electromagnetic, temperature variation, aging, etc.) influencing a DNN's functionality by changing its parameters (e.g., weights) or activation values during run-time.

To ensure a reliable DNN deployment, the first step is to extensively evaluate the performance and functionality of pre-trained DNNs against hardware faults. To achieve this objective, three main approaches are identified throughout the state-of-the-art, in a prior systematic literature review [22]: 1) Fault Injection (FI) methods in which faults are injected into the target system and simulated, 2) Analytical methods where faults effects are mathematically analyzed, and 3) Hybrid methods that combine FI and analytical methods.

It was observed that the majority of existing research works adopt FI (based on simulation, emulation, or irradiation). In FI experiments, faults can be accurately modeled, and the behavior of a system is evaluated in the presence of faults. However, given the growing size of emerging DNNs and their accelerators [15], [24], obtaining a fully precise evaluation is unfeasible and impractical.

Throughout the literature, multiple research works are presented to significantly reduce the simulation complexity of FI experiments for DNNs while maintaining statistical accuracy. It includes software simulation [25], [26], [27], [28], or hardware emulation [29], [30], [31]. Nonetheless, any FI experiment requires a certain level of statistical confidence, which is obtained by a considerably high number of repetitions and a multitude of fault locations [26]. Therefore, FI-based approaches for reliability assessment are inherently unscalable and take days and weeks using powerful computing resources such as GPU.

On the other hand, analytical approaches are presented to tackle the scalability issue. Nonetheless, they cannot provide reliability-oriented metrics including Vulnerability Factors (VFs) which is an essential metric for reliability evaluation. Moreover, the accuracy of analytical methods is not comparable to that of FI-based methods. To tackle the existing issues in the literature, a prior semi-analytical method named DeepVigor [23] is proposed as an alternative to simulation-based FI. DeepVigor provides accurate VF for bits, neurons, and layers of CNNs demonstrated to be faster than FI by utilizing a fault propagation analytical method. However, it analyzes all neurons in a CNN, implying a huge search space to obtain vulnerability values, leading to a scalability issue for large and deep emerging CNNs.

In this paper, we propose a scalable, fast, and accurate alternative to FI named DeepVigor+, which provides VF for layers and models of DNNs. DeepVigor+ takes advantage of an optimal fault propagation analysis within neurons and entire DNNs to derive VFs in an optimized way. To the best of our knowledge, DeepVigor+ is the first scalable semi-analytical alternative to FI with a comparable accuracy for resilience

analysis of DNNs in the literature. The contributions of this paper are as follows:

- Introducing a scalable, fast and accurate resilience analysis method for DNNs called DeepVigor+ for deriving VFs for DNNs' layers and models by analyzing both parameters and activations as well as by exploiting an optimal error propagation analysis. DeepVigor+ conducts a novel statistical approach based on stratified sampling unleashing a fast and accurate resilience analysis for large and deep emerging DNNs,
- Extensively demonstrating the effectiveness of DeepVigor+ by examining its error compared to FI, leading to meeting a 1% mean absolute error in obtaining VF. Furthermore, its scalability is evidenced against statistical FI, resulting in 14.9 to 26.9 times fewer simulations than a cutting-edge state-of-the-art statistical FI approach. Derived VF by DeepVigor+ can provide the possibility of reliability comparison and visualization between and within various DNN models in a few minutes for deep and large DNNs.

DeepVigor+ is presented as an open-source tool (<https://github.com/mhahmadilivany/DeepVigor>), unlocking reliability analysis for emerging DNNs and enabling researchers to quickly assess their reliability and design and develop fault-tolerant DNNs.

Table I presents the abbreviations frequently used in the manuscript. In the rest of the paper, Section II highlights the gap by overviewing the related works on statistical FI as well as analytical methods. Section III presents the methodology of DeepVigor+ leading to fast and accurate reliability analysis for CNNs. Section IV explains how DeepVigor+ is implemented and describes the experiments, and their results are presented in detail in Section V to demonstrate the efficiency of DeepVigor+. Finally, Section VI concludes the paper.

TABLE I: Frequent abbreviations used in this manuscript.

Abbreviation	Description
DNN	Deep Neural Network
CNN	Convolutional Neural Network
FI	Fault Injection
SFI	Statistical Fault Injection
VF	Vulnerability Factor
CVF	Channel Vulnerability Factor
LVF	Layer Vulnerability Factor
MVF	Model Vulnerability Factor
OFMap	Output Feature Map
IFMap	Input Feature Map
VVSS	Vulnerability Values Search Space
EDM	Error Distribution Map
CVV	Candidate Vulnerability Value
VVR	Vulnerability Value Range
MAE	Mean Absolute Error

## II. RELATED WORKS: RESILIENCE ANALYSIS METHODS FOR DNNs

With the fast growth of emerging DNNs' size regarding their memory and computation requirements, their reliability analysis becomes prohibitively complex, time-consuming and resource-hungry. In a recent literature review [22], it has been observed that the majority of papers studying the reliability of

DNNs exploit a Fault Injection (FI) approach. Software-level simulation FI is widely adopted in reliability analysis due to its low design time and fast execution.

Multiple open-source tools for software-level simulation-based reliability analysis are proposed in the literature, and the most adopted ones include PytorchFI [27] and TensorFI [32], [33], enabling FI simulations in PyTorch and TensorFlow respectively. These software-level FI tools support various fault models and provide different metrics for the resilience analysis of DNNs regarding parameters and activations.

Any FI simulation requires multiple simulations while a random set of parameters/activations are faulty and propagated through the forward execution of a DNN. Then, the erroneous outputs are observed, and reliability metrics are acquired. The number of simulations affects the accuracy of the obtained metrics. In exhaustive FI, all possible bitflips in the fault space are flipped individually, leading to a huge simulation space, which is impractical since DNNs possess millions of parameters and activations. Statistical Fault Injection (SFI) attempts to reduce the number of simulations based on statistical analysis, while guaranteeing a certain maximum error margin.

For conventional computing hardware, the number of simulations in an SFI experiment used to be specified by Eq. (1), where  $n$  is the number of samples,  $N$  is total fault space,  $e$  is the error and  $t$  is determined based on the expected confidence-level [34].

$$n = \frac{N}{1 + e^2 \times \frac{N-1}{t^2 \times p(p-1)}} \quad (1)$$

However, it is shown that applying Eq. (1) to the entire DNN does not result in statistically accurate results [26]. Authors in [26] introduced multiple methods to improve the accuracy of SFI as well as to reduce the number of simulations. Accordingly, layer-wise SFI, data-unaware SFI and data-aware SFI were presented, which generally apply Eq. (1) to each layer separately. Data-unaware SFI and data-aware SFI methods consider FI at the bit level to improve the statistical experiments. In data-unaware  $p = 0.5$  for all bits in Eq. (1), whereas in data-aware SFI requires a pre-analysis to specify the  $p$  for each bit position in the data representation.

Yet, SFI requires hundreds of thousands of simulations in any FI method leading to a significantly long simulation time even with leveraging GPUs. Furthermore, the growth of emerging DNNs necessitates an increasing number of simulations. Therefore, reliability analysis requires a paradigm shift in resilience analysis. Analytical methods for reliability analysis of DNNs are proposed to address its scalability issue.

Throughout the literature, multiple techniques are proposed to obtain the resilience of CNNs based on non-FI approaches, called analytical methods [22]. Layer-wise Relevance Propagation (LRP) is proposed to derive the contribution of neurons to the classification output of CNNs expressing their criticality in the presence of faults and errors [35]. The gradient-based analysis is exploited in [36], [37], [38], [39], [40] to obtain the resilience of CNNs against faults. Nonetheless, gradients neither represent the impact of faults on misclassification nor result in a probabilistic outcome of faults' effect on outputs.

Also, faults may change the values significantly, while gradients represent small variations in erroneous values.

Therefore, the existing analytical approaches do not result in accurate metrics for the reliability analysis of DNNs. DeepVigor was proposed to address this gap in the literature to provide fast and accurate metrics for the resilience of CNNs against faults [23]. It provides a Vulnerability Factor (VF) for bits, neurons and layers in CNNs by acquiring vulnerability values for each neuron (i.e., output feature maps). Vulnerability values represent how much a fault should change the golden value of a neuron's output to misclassify CNN's golden classification. Although DeepVigor is demonstrated to be faster than FI due to its fault propagation analysis method, it requires a high execution time to obtain VFs. The reason is that DeepVigor attempts to analyze all neurons in a CNN as well as to find the vulnerability values in a huge space of numbers.

This paper proposes DeepVigor+, a new method to quickly obtain VF metrics for layers and DNN models addressing both scalability and accuracy of fault resilience analysis in the literature. DeepVigor+ employs an optimized error propagation analysis in neurons, assuming that a single fault might happen either at its inputs or weights, thus leading to effectively shrinking the search space for vulnerability values. Moreover, DeepVigor+ proposes a stratified sampling to further accelerate the process of resilience analysis without a tangible analysis accuracy mitigation, leading to obtaining VF in a few minutes, even for deep and large emerging DNNs.

### III. METHODOLOGY: SCALABLE AND ACCURATE RESILIENCE ANALYSIS FOR DNNs BY DEEPVIGOR+

In this section, the proposed resilience analysis method for DNNs, DeepVigor+, is presented. First, the fault model and its effect on 32-bit floating point values are described. Then, the mathematical model for fault propagation in DNNs is explained, which forms the basis for the DeepVigor+ analysis.

#### A. Fault Model

Transistor miniaturization leads to more efficient computational digital systems, whereas its reliability side-effects are becoming increasingly profound. With transistor scaling soft error rates increase significantly posing reliability concerns, in particular in the deployment of safety-critical applications [41], [42], [43]. Single Event Upset (SEU) due to soft errors may affect memory cells and flip a bit in a stored value. SEU in DNN accelerators affects either the parameters of a DNN (i.e., weights) or its activations (i.e., layers' inputs), which are stored in memory elements such as registers or on-chip memories [16], [22].

For reliability analysis, the multi-bit fault model is more realistic, however, it requires a huge fault space to consider all combinations, i.e.,  $3^{n-1}$  combinations where  $n$  is the number of bits. On the other hand, it is demonstrated that the single-bit fault model provides a high fault coverage of multiple-bit faults [44]. Therefore, analyzing the reliability of DNNs based on a single-bit fault model is valid for obtaining the VF of models. This fault model is in line with the other works in the literature [23], [25].

Therefore, in this paper we build our analysis based on the single-bit fault model in weights and activations separately. We assume that a single parameter or a single input to a layer is faulty which is propagated to the output of the corresponding layer. By mathematical analysis, we model the fault propagation to the output of neurons and DNNs, resulting in calculating VF for them.

### B. Single Fault Analysis in 32-bit Floating-Point

To model the behavior of faults for the analysis, we assume that at an inference, a single fault may influence the value of a single input activation to a neuron or a single parameter in a CNN. First, we analyze the effect of a single bitflip on the 32-bit floating-point data representation to comprehend how a value might change due to a single fault. IEEE-754 32-bit floating-point data type is shown in Fig. 3. It contains 1 sign bit, 8 exponent bits, and 23 fraction bits, and represents a number based on Eq. (2).

$$number = (-1)^{sign} \times 2^{E-127} \times (1 + \sum_{i=0}^{23} b_{23-i} \times 2^i) \quad (2)$$

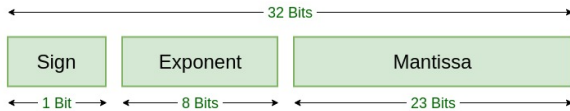


Fig. 3: 32-bit floating point IEEE-754 data representation.

In this regard, we consider the following lemmas:

- *Lemma 1:* Any bitflip from 1 to 0 in a value decreases the value as  $\epsilon$  while  $\epsilon < 0$ , and any bitflip from 0 to 1 increases it as  $\epsilon$  while  $\epsilon > 0$ .
- *Lemma 2:* In the 32-bit floating-point data representation, an error ( $\epsilon$ ) induced to a value ( $x$ ) by a bitflip in bit  $i$  can be represented as in Eq. (3), whether the bitflip is in sign bit ( $2 \times x$ ), exponent bits ( $2^i \times x$ ), or mantissa bits ( $2^i$ ), as stated in [45], [46].

$$\begin{cases} x_{faulty} = x + \epsilon \\ \epsilon \in \{2 \times x, 2^{i-23} \times x, 2^i\} \end{cases} \quad (3)$$

- *Lemma 3:* To unify the analysis of the error induced to a value by a single bitflip, we can approximate  $\epsilon$  by representing it as a power of two, for each section of the data representation, as follows:
  - 1) Sign: approximate  $\epsilon$  as  $\pm 2^{\log_2(2 \times x)}$ .
  - 2) Exponent: approximate  $\epsilon$  as  $\pm 2^{i-23}$ , assuming that  $x$  is a small value.
  - 3) Mantissa: approximate  $\epsilon$  as  $\pm 2^i$ .

In all cases,  $\epsilon$  can be approximated as the nearest value of the power of two to the actual  $\epsilon$ . This approximation can lead to a unified representation for  $\epsilon$ . To that end,  $\epsilon$  might be negative or positive (based on Lemma 1) and might be small or big (based on Lemma 2). Eventually,

we can express it as a unified representation as shown in Eq. (4).

$$\epsilon \approx \pm 2^\rho; \rho \in \{\pm 1, \pm 2, \pm 3, \dots\} \quad (4)$$

- *Lemma 4:* When a faulty value is used in a multiplication operation in CNNs, the erroneous output can also be approximated. It has been observed that the parameters in CNNs are mainly distributed around 0 and in the range of  $[-1, 1]$  [47]. In order to approximate the error of multiplying two values when one of them is faulty, we can analyze it based on Eq. (5), where  $x$  and  $y$  are fault-free values and  $x'$  is the faulty value after a bitflip in  $x$ .

$$\begin{aligned} \text{let : } & x' = x + \epsilon \\ \text{then : } & x' \times y = x \times y + \epsilon \times y \\ & \Rightarrow x' \times y = x \times y + \delta \end{aligned} \quad (5)$$

In Eq. (5), when  $x$  is a small value,  $\delta \approx 0$ . Since most values in CNNs' operations are close to 0, the erroneous values in multiplications in a CNN can be approximated based on the unified error representation, as shown in Lemma 3 and Eq. (4).

### C. Single Fault Error Propagation in DNNs

We analyze the single bitflip error propagation in CNNs considering their effect on the values of numbers. Each neuron in a convolutional (CONV) layer operates as shown in Eq. (6), where the Output Feature Map (OFMap) in  $l$ th layer and  $k$ th channel is obtained by the summation of multiplications between weights ( $\hat{w}$ ) and Input Feature Map (IFMap,  $\hat{x}$ ) plus bias ( $b$ ). In CONV layers,  $\hat{w}$  and  $\hat{x}$  are 3-Dimensional (3D)  $c_{in} \times n \times n$  arrays, where  $c_{in}$  is the number of inputs channels to the layer, and  $n$  is the kernel size.

$$OFMap_k^l(\hat{x}, \hat{w}, b) = \left( \sum_{i=0}^{c_{in}} \sum_{j=0}^n \sum_{k=0}^n x_{ijk} \times w_{ijk} \right) + b \quad (6)$$

Here, we assume that a fault affects a single IFMap in a single neuron, thus, it produces a single erroneous OFMap. Supposing that a fault occurs in an IFMap  $x_{ijk}$ , represented as  $x'_{ijk}$ . The fault introduces an error  $\epsilon$  to the fault-free value of  $x_{ijk}$ . Therefore, it can be expressed in Eq. (7).

$$x'_{ijk} = x_{ijk} + \epsilon \quad (7)$$

Hence, once a bitflip occurs in  $\hat{x}$  in Eq. (6), the partial multiplication is computed in Eq. (8). In this equation, the term  $x_{ijk} \times w_{ijk}$  represents the fault-free multiplication, and  $\epsilon \times w_{ijk}$  is an added error to the output by a fault which can be represented as  $\delta$ .

$$\begin{aligned} x'_{ijk} \times w_{ijk} &= (x_{ijk} + \epsilon) \times w_{ijk} \\ &= x_{ijk} \times w_{ijk} + \epsilon \times w_{ijk} \\ &= x_{ijk} \times w_{ijk} + \delta \end{aligned} \quad (8)$$

Consequently, the erroneous OFMap can be expressed in a way that it is the summation of the fault-free OFMap and  $\delta$ , while the single faulty IFMap in  $\hat{x}$  can be in any index of the corresponding 3D array. Considering Lemma 4, the induced error at the neuron's OFMap can be expressed in Eq. (9).

$$\begin{aligned} OFMap_k^l(\hat{x}', \hat{w}, b) &= OFMap_k^l(\hat{x}, \hat{w}, b) + \delta \\ \delta &\approx \pm 2^p; \rho \in \{\pm 1, \pm 2, \pm 3, \dots\} \end{aligned} \quad (9)$$

On the other hand, when a fault occurs in a weight, it has the same effect on a single neuron's output. However, the same faulty weight in the corresponding CONV layer is used by all neurons in the layer, as filters slide over all IFMaps. Therefore, it results in an output channel in which all OFMaps are erroneous, as shown in Fig. 4. Considering Lemma 4, the fault propagation for an output channel can be expressed in Eq. (10).

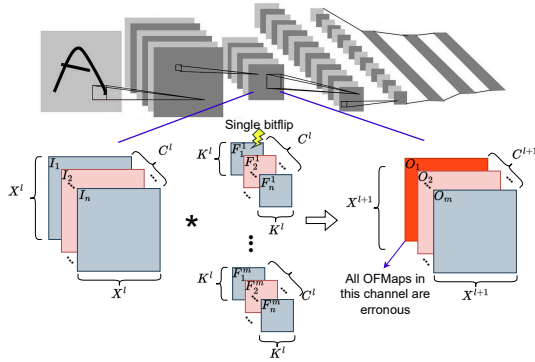


Fig. 4: Fault propagation in a CNN in the case of a single bitflip in a weight.

$$\begin{aligned} Out\_Channel_k^l(\hat{x}, \hat{w}, b) &= \hat{x} * \hat{w} + b \\ Out\_Channel_k^l(\hat{x}, \hat{w}', b) &= \hat{x} * \hat{w} + b + \epsilon * \hat{x} \\ Out\_Channel_k^l(\hat{x}, \hat{w}', b) &= Out\_Channel_k^l(\hat{x}, \hat{w}, b) + \delta \\ \delta &\approx \pm 2^p; \rho \in \{\pm 1, \pm 2, \pm 3, \dots\} \end{aligned} \quad (10)$$

Based on the aforementioned theoretical analysis, to analyze the effect of single faults on CNNs, regardless of the fault occurrence in activations or weights, we only need to identify an added value  $\delta$  (as a power of two) at the output of the target neuron/channel where it misclassifies the golden class of the CNN for each input image.

#### D. DeepVigor+: Fault Resilience Analysis for DNNs

In this section, the steps of DeepVigor+ are presented. Fig. 5 illustrates the steps of the DeepVigor+ methodology for fault resilience analysis of DNNs against single faults. The method's objective is to provide the Vulnerability Factor (VF) for layers and the entire DNN model when a single fault happens in activations or weights.

The inputs of the method are a pre-trained CNN and validation data in a dataset. During the analysis, an OFMap or output channel is targeted, and multiple steps are taken to provide the VF metrics:

- 1) Single Bitflip Analysis: constructs a search space for possible vulnerability values and produces a distribution of erroneous values based on the approximations in Eq. (9) and (10),
- 2) Vulnerability Values Identification: obtains vulnerability values for the target OFMap/channel
- 3) Obtaining Vulnerability Factor: exploits identified vulnerability values and error distribution to provide VF for the target neuron/channel.

By obtaining the VF for the analyzed neurons and filters in a DNN, the VF for layers and the entire DNN can be derived. The details of each step are explained in the following. Noteworthy that each step presents a detailed description for analyzing a target neuron and then briefly links it to weights in filters.

**Step 1 - Single Bitflip Analysis:** As mentioned above, single faults at the inputs of a neuron are considered. This step conducts bitflips in the input activations of the target neuron to construct Vulnerability Values Search Space (VVSS) and Error Distribution Map (EDM) for the target neuron. VVSS is a set of candidate values representing all possible  $\delta$  in Eq. (9). In other words, VVSS represents output errors produced by single bitflips in any bit locations of the inputs of the target neuron. EDM represents the distribution of  $\delta$  in Eq. (9) throughout the approximated  $\delta$  values with a power of two.

Obtaining VVSS and EDM requires performing a single bitflip for each input and multiplying it by its corresponding weight as shown in Eq. (8). Nonetheless, it is an exhaustive operation with high time complexity. This complexity can be remarkably reduced by leveraging Algorithm 1. In this algorithm, for each bitflip, we obtain all possible  $\delta$  produced at the output of the neuron for all inputs at once.

Since each input might be faulty separately, to produce all errors in a neural operation, we first flip the  $i$ th bit in all inputs

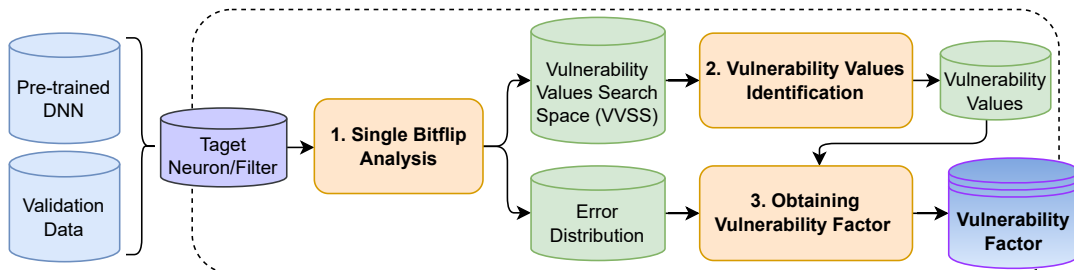


Fig. 5: An overview of the conducted steps in DeepVigor+.

(line 3) and then convert the binary representation to a value (line 4). Then, the difference of the *erroneous\_inputs* with the fault-free input is computed (line 5), which represents all possible errors at inputs ( $\epsilon$  in Eq. (8)) for all inputs added by a single bitflip in either of them. Then, a point-wise multiplication between the *erroneous\_inputs* and *weights* results in producing all possible errors ( $\delta$  in Eq. (9)) at the output (line 6).

---

**Algorithm 1** Error Analysis for a Neuron

---

**Input:** Target neuron’s inputs and weights as 3D matrices;

**Output:** All possible errors at the output;

Assume:  $\delta$  is the error added to each golden output; All values are in 32-bit floating-bit;

- 1: `binary_representation = float32_to_binary(inputs);`
  - 2: **for**  $i \in [0, 31]$  **do**:
  - 3:   `flip bit  $i$  in binary_representation;`
  - 4:   `erroneous_inputs =`  
    `binary_to_float32(binary_representation);`
  - 5:   `input_errors = erroneous_inputs - inputs;`
  - 6:   `output_errors_list.append(input_errors  $\odot$  weights);`
  - 7: **end for**;
- 

Algorithm 1 produces all errors at the output of the target neuron. Thereafter, based on the presented theory in the subsections III-B and III-C, we generate the distribution of all produced errors as an Error Distribution Map (EDM) based on the Candidate Vulnerability Values (CVVs) which are a set of numbers as a power of two, shown in Eq. (11). Based on the experimental observations, we limit the CVV in the analysis between  $-2^{10}$  and  $2^{10}$  for large values. The error values between  $-2^{-10}$  and  $2^{-10}$  are merged as their propagation effects on CNNs are negligible and masked.

$$CVV = \{\pm 2^\rho\}; \rho \in \{0, \pm 1, \pm 2, \pm 3, \dots, \pm 9, \pm 10\} \quad (11)$$

EDM contains the *distribution ratio* of the existing values over the values in *output\_errors\_list* in Algorithm 1, between each consecutive values in CVV, as shown in Eq. (12). EDM provides the ratio of error distribution with respect to each

candidate vulnerability value, demonstrating how much each CVV represents the produced errors at the output of the target neuron. Based on the EDM, each CVV whose *distribution ratio* is not zero, is added to the Vulnerability Value Search Space (VVSS). This means that VVSS contains a subset of CVV that are the approximated errors produced by single faults in the inputs and might lead to misclassification at the output of the CNN.

$$\forall i \in CVV; \text{distribution\_ratio}_i = \frac{\text{count}(CVV_{i-1} < \text{output\_errors\_list} < CVV_i)}{\text{count}(\text{output\_errors\_list})} \quad (12)$$

The process of single bitflip analysis for a target filter is similar to the one for a neuron. Nonetheless, in the case of a bitflip in a filter, all OFMaps in an output channel are affected (as described in subsection III-C and Eq. (10)). Therefore, this step is performed separately on every bit of all weights in the target filter, so that VVSS and EDM for the corresponding filter are obtained.

**Step 2: Vulnerability Values Identification:** This step exploits VVSS to identify the vulnerability values for the target neuron (i.e., OFMap) by exploring its constructed VVSS. As mentioned, VVSS represents output errors induced by a single fault occurring at the inputs of the target neuron. The objective is to identify the *maximum negative* and *minimum positive* vulnerability values among the existing ones in VVSS for a neuron that misclassify the DNN’s outputs from its golden classification for each input data.

To explore the vulnerability values efficiently, we divide them into four different exploration spaces:

- 1)  $VVSS_{[-\infty, -1]}$ : contains CVVs between  $[-\infty, 1]$  that have a non-zero distribution ratio.
- 2)  $VVSS_{(-1, 0)}$ : contains CVVs between  $(-1, 0)$  that have a non-zero distribution ratio.
- 3)  $VVSS_{(0, 1)}$ : contains CVVs between  $(0, 1)$  that have a non-zero distribution ratio.
- 4)  $VVSS_{[1, +\infty]}$ : contains CVVs between  $[1, +\infty]$  that have a non-zero distribution ratio.

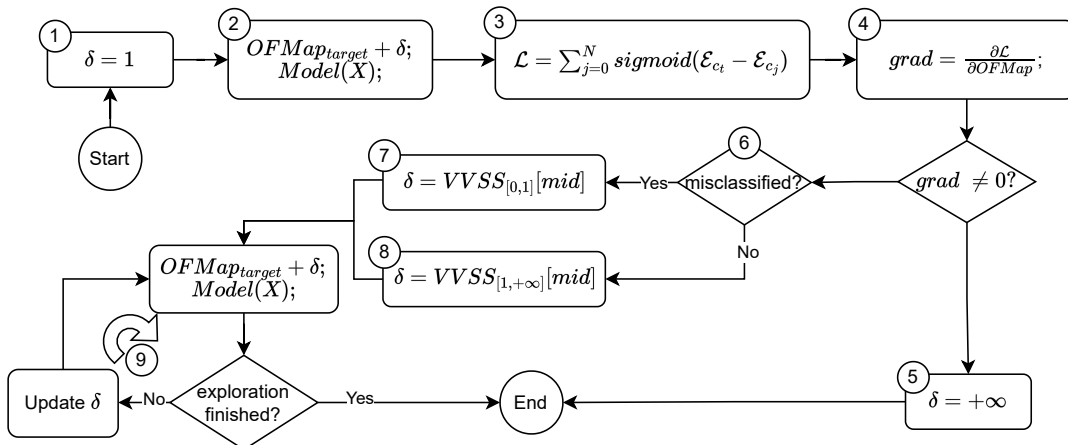


Fig. 6: Vulnerability value identification for a target neuron with a single input data for positive errors.

The flowchart in Fig 6 illustrates the algorithm of vulnerability value identification for *positive vulnerability values* for a single input data  $\mathbf{X}$ . In this flowchart,  $\delta$  is the vulnerability value added to the target OFMap. First,  $\delta$  equals 1 (box 1) is added to the target OFMap. Thereafter, the forward pass of the CNN is performed to obtain its output logits ( $\mathcal{E}$ ) while a neuron is erroneous (box 2).

In box 3, a loss function  $\mathcal{L}$  is calculated to obtain the effect of added  $\delta$  to the target OFMap on the output classes based on the summation of the differences between all output class's logits from the golden class. In this loss function,  $\mathcal{E}_{c_t}$  represents the erroneous output logit of the golden top class and  $\mathcal{E}_{c_j}$  is the erroneous output logit of any other class.

In box 4, the gradient of loss function  $\mathcal{L}$  w.r.t. the target OFMap is calculated to check if the CNN might be misclassified or not, when the target OFMap is erroneous. If the gradient is 0, faults producing positive deviation in the corresponding neuron do not lead to misclassification. In this case, the neuron's vulnerability value is considered the biggest CVV assumed value for positive numbers (i.e.,  $2^{10}$ ) in box 5, and the algorithm ends. If the gradient is not equal to 0, a value can be found for  $\delta$  in the target OFMap which misclassifies the DNN. The rest of the algorithm attempts to find the minimum positive  $\delta$  in VVSS.

In box 6, it is examined if the CNN misclassifies the input from its golden classification when  $\delta = 1$  for the target neuron, determining the initialization for  $\delta$  in the next steps. If the input is misclassified when  $\delta = 1$ , it means that its vulnerability value is less than 1 and we should explore  $VVSS_{(0,1)}$  (box 7), otherwise,  $VVSS_{[1,+\infty)}$  should be explored (box 8). In the case of exploring  $VVSS_{(0,1)}$ ,  $\delta$  is set to the middle element of the set, and if it does not misclassify the golden output, the next bigger CVV should be explored. This process continues until the first value which misclassifies the output is found (loop 9). The final positive vulnerability value ( $\delta^+$ ) for the target neuron is the minimum value in positive VVSS that does not misclassify the input for CNN from its golden classification.

To identify the maximum negative vulnerability value ( $\delta^-$ ) that does not misclassify the input from its golden classification, the same procedure is conducted to explore negative values in VVSS. As a result, the Vulnerability Value Range (VVR) for the corresponding neuron is obtained and is expressed in Eq. (13). VVR represents all induced error values to the outputs of a neuron leading to a misclassification. Noteworthy that since bitflips in 32-bit floating-point might lead to large values, we assumed that any value larger than  $2 * 10$  and less than  $2^{-10}$  are critical for CNNs, therefore, these values represent  $+\infty$  and  $-\infty$  respectively.

$$VVR = (-\infty, \delta^-] \cup [\delta^+, +\infty) \quad (13)$$

The step of vulnerability values identification for a target filter is similar to the one for a neuron. It is conducted similarly to the illustrated flowchart in Fig. 6 to obtain VVR for the corresponding output channel resulting in VVR for each target channel in a DNN.

**Step 3: Obtaining Vulnerability Factors:** As mentioned, an Error Distribution Map (EDM) is obtained for the target

neuron in step 1, representing the distribution ratio for each vulnerability value. On the other hand, the Vulnerability Value Range (VVR) is obtained in step 2. This step aims to map VVR to EDM to provide the VF for the target neuron, expressing the probability of misclassification in the case of a single bitflip in its inputs.

Fig. 7 depicts how VF can be obtained by mapping VVR to aggregated EDM. Aggregated EDM represents the summation of the *distribution ratio* for all values less than a CVV. As shown in Fig. 7, all values between ( $\delta^-, \delta^+$ ) are non-vulnerable meaning that if an error deviates the OFMap as big as any value in this range, it will not misclassify the golden output. Otherwise, the error value is vulnerable leading to a misclassification.

VF is obtained by subtracting the distribution ratio of the minimum positive vulnerability value ( $\delta^+$ ) and the maximum negative vulnerability value ( $\delta^-$ ) as shown in Eq. (14). This equation expresses what portion of all errors produced at the output are critical for the CNN in terms of misclassification which is equivalent to the probability that a fault misclassifies the CNN's output.

$$VF_{target\_neuron} = 1 - (distribution\_ratio_{\delta^+} - distribution\_ratio_{\delta^-}) \quad (14)$$

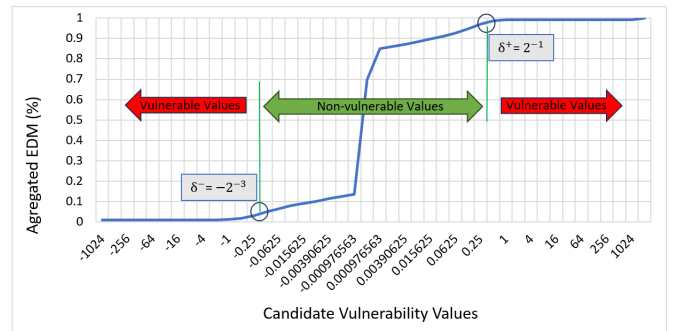


Fig. 7: Mapping obtained Vulnerability Value Range (VVR) to aggregated Error Distribution Map (EDM) for VF calculation.

The VF for a filter is obtained similarly. the EDM and VVR for the target filter are obtained in the previous steps. In this step, they are exploited to provide the VF for the target filter. Deriving the VF for individual neurons and filters leads to obtaining the VF for CONV layers and the entire CNN model. Since the analysis is performed for neurons and filters separately, it can provide separate VF for layers and for the entire model based on filters and neurons. The Layer Vulnerability Factor (LVF) is the average of VF for all activations/filters, and the Model Vulnerability Factor (MVF) is the average of LVFs within it.

Furthermore, to obtain the total MVF of the entire model using the obtained detailed VFs based on the activations and filters analysis, Eq. (15) is introduced, where  $L$  is the total number of layers in a CNN,  $N_l$  and  $W_l$  are the total number of output activations and weights in layer  $l$ . This equation is a layerwise weighted average of LVFs throughout the layers of a CNN including both activations and filters vulnerability

analysis, leading to the MVF for the entire model, representing the probability of misclassification if a fault occurs either in activations or weights.

$$MVF_{total} = \frac{\sum_{l=1}^L (\frac{N_l}{N_l+W_l} \times LVF_{act_l} + \frac{W_l}{N_l+W_l} \times LVF_{weight_l})}{L} \quad (15)$$

### E. Stratified Random Sampling for Vulnerability Analysis:

The DeepVigor+ analysis can be conducted for all neurons/filters in a CNN. However, performing a complete analysis is obstructive and time-consuming, in particular for very deep and emerging CNNs. To address the scalability issue in resilience analysis for huge CNNs, we exploit the stratified sampling concept to reduce the sampling size for statistical DeepVigor+ analysis. Stratified random sampling is a method to increase the accuracy of estimation in sampling by dividing the population into subgroups called *strata* and random samples can be selected within them [48].

In DeepVigor+, the analysis is performed layer by layer. To take the benefits of stratified sampling for reducing the execution time of the analysis, we assume that each output channel in a layer is one stratum. Thereafter, a portion of all output channels specified by *channel\_sampling\_ratio* is considered and some random channels are selected. Within each channel, the number of analyzed neurons is determined by the  $\log_2(\#neurons)$  in the target channel, which is selected randomly. Therefore, the number of analyses can be described with Eq. (16).

$$\#analyzed\ neurons = \sum_{l \in layers} [channel\_sampling\_ratio \times out\_channel_l] \times \log_2(\#neurons_{channel}^l) \quad (16)$$

## IV. EXPERIMENTAL SETUP

### A. DeepVigor+ Implementation

DeepVigor+ is fully implemented using Python and the Pytorch library. The source code of DeepVigor+ is fully open-source in <https://github.com/mhahmadilivany/DeepVigor> as a tool to enable researchers and engineers to adopt it for the resilience analysis of DNNs. The user can obtain the VF for the CONV layers of a target CNN based on analyzing neurons or weights by determining it through some inputs. User can specify the following inputs for the analysis:

- Target pre-trained CNN: the tool loads the pre-trained set of weights.
- Dataset: the tool loads the validation data from the dataset.
- Analysis method: the tool performs resilience analysis for neurons (OFMaps) or filters (weights).
- Sampling method: the tool performs either complete analysis or stratified random sampling based on *channel sampling ratio*.
- Channel sampling ratio: in the case of stratified random sampling, the channel sampling ratio should be specified.

With the determined inputs, the tool performs the analysis and outputs the Layer Vulnerability Factor (LVF) for each layer and the Model Vulnerability Factor (MVF) for the entire CNN model. In the paper, we perform the DeepVigor+ analysis on one batch of 100 images in the test set. Note, that all experiments consider 32-bit floating-point data representation.

### B. Validating DeepVigor+

We use Fault Injection (FI) to validate the results of DeepVigor+. To that end, we validate the VF for channels by analyzing filters of CNNs using complete DeepVigor+ and weights FI. In this regard, before an inference, a random 3D filter in a specified layer is selected. In the FI campaign, one bit of one weight in the target filter is flipped considering 32-bit floating-point data representation and the inference is performed on the same data as the DeepVigor+ analysis was conducted. The same FI process is carried out for all bits of weights in the target filter resulting in the Channel Vulnerability Factor (CVF) calculated by the ratio of output misclassifications compared to the golden outcomes. The obtained CVF in FI for each channel is compared with the one in complete DeepVigor+ for the corresponding channel, and their absolute errors are reported. In all DNNs under the experiment, 15% of all channels throughout the CONV layers are passed through the FI campaign for validation.

To show the accuracy of the result in exploited stratified sampling in DeepVigor+, we compare the obtained VF for channels (CVF) and layers (LVF) in sampling DeepVigor+ vs. complete DeepVigor+ for both activations and filters. The absolute difference between obtained VFs is derived to show the VF estimation in sampling analysis. In order to achieve more accurate results, different *channel\_sampling\_ratios* are experimented including 5%, 10%, 15%, and 20%. Since neurons and channels are selected randomly in the stratified sampling, each sampled analysis is repeated 50 times and the maximum and mean absolute errors are reported.

Furthermore, to show the efficiency of DeepVigor+ analysis, we present the number of simulations for DeepVigor+ and how it outperforms FI. First, we compare the number of simulations for DeepVigor+'s complete analysis against exhaustive FI. Also, we compare the number of simulations for sampling DeepVigor+ with state-of-the-art Statistical FI (SFI) methods for CNNs proposed in [26], considering layer-wise SFI, data-unaware SFI, and data-aware SFI. Finally, the paper demonstrates the execution time for the complete and sampling DeepVigor+ on an NVIDIA A100 GPU to showcase the efficiency of the proposed method.

### C. DNNs Under Study

In this paper, Deepvigor+ is executed and validated on six pre-trained DNNs using various datasets. DNNs under analysis include VGG-11 trained on CIFAR-10, VGG-16, ResNet-18-C and MobileNetV2 trained on CIFAR-100, ResNet-18-I and ResNet-34 trained on ImageNet. The baseline accuracy, number of channels and neurons for each DNN are shown in Table II. All experiments in this paper are performed on an NVIDIA A100 GPU accompanied by AMD EPYC 7742 64-core CPU.

TABLE II: The DNNs under study for DeepVigor+ validation.

DNN	Dataset	Baseline accuracy	# of conv layers	# of channels	# of neurons
VGG-11	Cifar-10	92.52%	8	2,752	232,448
VGG-16	Cifar-100	66.97%	13	4,224	185,344
ResNet-18-C	Cifar-100	70.26%	20	4,800	666,624
MobileNetV2	Cifar-100	61.27%	54	17,188	854,064
ResNet-18-I	ImageNet	69.19%	20	4,800	2,182,656
ResNet-34	ImageNet	73.04%	36	8,512	3,437,056

## V. EXPERIMENTAL RESULTS

### A. DeepVigor+ Accuracy with FI

To analyze the accuracy of the obtained VFs by DeepVigor+, we perform fault injection experiments on 15% of randomly selected channels in all DNNs in Table II and present the Mean Absolute Error (MEA), as described in subsection IV-B. Table III presents the MEA results comparing the Channel Vulnerability Factor (CVF) by the complete DeepVigor+ filters analysis vs full FI into 15% of channels in each DNN. Noteworthy that the acceptable mean error is 1% [26].

The results in Table III indicate that the mean absolute error by DeepVigor+ compared to exact FI throughout the DNNs is between 0.819% to 0.978%, i.e., always less than 1%. These results demonstrate that DeepVigor+ is able to provide precise VFs and meets the expectation of an acceptable error with respect to exhaustive FI experiments.

TABLE III: Absolute error for CVF in DeepVigor+ and fault injection for 15% of the channels in DNNs.

DNN	VGG-11	VGG-16	ResNet-18-C	Mobile-NetV2	ResNet-18-I	ResNet-34
Mean Absolute Error (%)	0.819	0.938	0.933	0.874	0.978	0.878

The main sources of error in VF calculation in DeepVigor+ are:

- 1) As discussed in subsection III-C, DeepVigor+ approximates the error propagation in neurons based on the values of power of 2. This error approximation introduces an error to the resilience analysis which is also reflected in VF calculation.
- 2) DeepVigor+ assumes that bitflips resulting in big values are critical for DNNs and the *distribution ratio* for large values are always considered critical. However, in some cases, these values don't result in misclassification. This phenomenon is another reason for a minor difference between the VF by FI and DeepVigor+.

### B. Sampling Analysis vs. Complete Analysis

This subsection presents the results for sampling DeepVigor+ and compares its VF results against the complete analysis to show how accurate sampling DeepVigor+ is. Channel Vulnerability Factor (CVF) and Layer Vulnerability Factor (LVF) are derived as described in subsection III-D and the maximum and mean absolute error for obtained CVFs and LVFs in complete and sampling DeepVigor+ for neurons and filters

are presented separately. In sampling DeepVigor+, *channel sampling ratio* is explored.

Table IV indicates the absolute error results over various *channel sampling ratio* for DNNs under study, in both neurons and filters analysis. Each sampling analysis is repeated 50 times to observe the effect of random selections in stratified sampling. Based on the results, the minimum absolute error throughout the experiments for both CVF and LVF is very close to 0. As observed, the difference between obtained CVFs and LVFs throughout the results is minimal, demonstrating the effectiveness of the exploited stratified sampling.

In all experiments, the Mean Absolute Error (MAE) for CVF does not vary since the sampling method within channels is similar (i.e., the logarithm of the number of OFMaps). Also, it is observed that the MEA CVF is less than 0.065% in all experiments for both activations and filters sampling analysis. It means that the averaged VF for the logarithm-based random sampling within each channel results in a highly accurate CVF. This phenomenon is a result of the unified distribution of weights within a channel in a pre-trained DNN. The maximum observed error in neuron analysis is 0.004% to 1.443% throughout DNNs, whereas the mean error remains low, meaning that for most of the channels, obtained CVFs are highly accurate leading to an overall high accuracy for obtained CVFs.

On the other hand, *channel sampling ratio* directly affects the accuracy of LVF calculations. As observed in Table IV, LVF error decreases with the increase of *channel sampling ratio*. Considering both MEA and maximum error for LVF, a 10% *channel sampling ratio* can guarantee a minimal error for VF calculations. Based on the MEA of complete DeepVigor+ compared to exhaustive FI Table III, sampling DeepVigor+ with 10% channel sampling ratio ensures that all the overall error of obtained VFs for all DNNs will be lower than 1%.

In conclusion, the proposed stratified sampling in DeepVigor+ results in highly accurate VF for channels and layers obtained from both activations and filter analysis with a *channel sampling ratio* of 10%. Sampling DeepVigor+ results in a higher error than state-of-the-art statistic FI approaches such as data-aware and data-unaware, yet it meets the requirement of average error for resilience study which is 1%.

### C. Run-Time and Scalability Investigation

To show the excellence of DeepVigor+ in terms of complexity, scalability and execution time against FI, first, we investigate the complexity of each based on the required number of simulations (i.e., forward pass executions) to obtain VF. Then we present the execution time for the complete and sampling DeepVigor+ on an NVIDIA A100 GPU.

Exhaustive FI is the most accurate method for determining precise VFs. In exhaustive FI, the required number of simulations equals the number of activations/weights times bit-width (i.e., 32 bits). Therefore, its complexity is proportional linearly to the size of DNNs. Whereas the complete DeepVigor+ analysis estimates VFs with high accuracy and significantly lower complexity. Although its complexity is affected by the size of DNNs, DeepVigor+ analysis exploits various

TABLE IV: Average absolute error analysis over 50 executions for sampling DeepVigor+ compared to complete analysis.

DNN	channel sampling ratio	Activations analysis				Filters analysis			
		MAE CVF	Max error CVF	MAE LVF	Max error LVF	MAE CVF	Max error CVF	MAE LVF	Max error LVF
VGG-11	5%	0.0004%	0.011%	0.0010%	0.012%	0.064%	0.171%	0.019%	0.125%
	10%	0.0004%	0.008%	0.0008%	0.008%	0.064%	0.148%	0.015%	0.097%
	15%	0.0004%	0.004%	0.0007%	0.007%	0.063%	0.130%	0.011%	0.083%
	20%	0.0004%	0.006%	0.0007%	0.007%	0.063%	0.128%	0.008%	0.076%
VGG-16	5%	0.037%	0.141%	0.033%	0.250%	0.045%	0.216%	0.017%	0.183%
	10%	0.038%	0.144%	0.022%	0.188%	0.044%	0.116%	0.010%	0.094%
	15%	0.038%	0.118%	0.018%	0.168%	0.043%	0.137%	0.008%	0.064%
	20%	0.038%	0.130%	0.015%	0.140%	0.043%	0.141%	0.007%	0.065%
ResNet-18-C	5%	0.029%	0.097%	0.054%	0.633%	0.045%	0.153%	0.016%	0.137%
	10%	0.029%	0.092%	0.038%	0.386%	0.045%	0.123%	0.011%	0.076%
	15%	0.029%	0.093%	0.031%	0.272%	0.045%	0.127%	0.010%	0.083%
	20%	0.029%	0.071%	0.026%	0.300%	0.045%	0.124%	0.008%	0.085%
MobileNetV2	5%	0.031%	1.443%	0.079%	2.803%	0.030%	0.893%	0.013%	0.983%
	10%	0.033%	0.841%	0.053%	1.252%	0.030%	0.401%	0.009%	0.372%
	15%	0.032%	0.586%	0.044%	0.742%	0.030%	0.468%	0.007%	0.346%
	20%	0.032%	0.465%	0.037%	0.720%	0.030%	0.401%	0.006%	0.320%
ResNet-18-I	5%	0.005%	0.071%	0.007%	0.168%	0.041%	0.115%	0.016%	0.114%
	10%	0.005%	0.070%	0.005%	0.212%	0.041%	0.096%	0.010%	0.061%
	15%	0.005%	0.054%	0.004%	0.108%	0.041%	0.083%	0.008%	0.062%
	20%	0.005%	0.045%	0.003%	0.082%	0.042%	0.089%	0.006%	0.032%
ResNet-34	5%	0.003%	0.061%	0.005%	0.140%	0.045%	0.136%	0.016%	0.087%
	10%	0.003%	0.059%	0.003%	0.084%	0.045%	0.127%	0.011%	0.097%
	15%	0.003%	0.054%	0.002%	0.089%	0.046%	0.122%	0.009%	0.080%
	20%	0.003%	0.048%	0.002%	0.063%	0.045%	0.120%	0.007%	0.061%

optimizations to reduce the number of simulations resulting in significantly lower complexity than exhaustive FI. This is evidenced by the results in Table V where the required number of simulations is compared between Exhaustive FI and complete DeepVigor+ analysis, for activations and filters separately.

TABLE V: Number of simulations for exhaustive FI vs complete DeepVigor+ for activations and filters analysis.

DNNs	Activations		Filters	
	Exhaustive FI	DeepVigor+	Exhaustive FI	DeepVigor+
VGG-11	7,438,336	1,636,414	294,967,296	11,035
VGG-16	5,931,008	2,018,447	470,734,848	13,704
ResNet-18-C	21,331,968	3,387,189	357,095,424	15,906
MobileNet-V2	27,330,048	3,029,125	74,176,512	42,234
ResNet-18-I	69,844,992	20,730,314	357,341,184	23,450
ResNet-34	109,985,792	28,821,489	680,564,736	43,098

As observed, for each DNN, DeepVigor+ complete analysis requires significantly lower executions either in activations or filters analysis. Throughout the results, activations analysis by complete DeepVigor+ is 2.93 to 9.02 times faster than exhaustive FI. According to our detailed investigations, activations analysis by DeepVigor+ requires 6 forward simulations per neuron, on average, throughout the DNNs under study. In this regard, the introduced loss function to obtain the vulnerability values (box 4 in Fig 6) contributes to skipping the analysis for up to 26% of neurons. Moreover, the vulnerability value can be obtained by a single forward simulation for up to 55% of neurons due to separating VVSS exploration (boxes 7 and 8 in Fig. 6).

In the complete filters analysis, the DeepVigor+ fault propagation modeling implies a huge impact on the number of simulations in the orders of magnitude. DeepVigor+ can derive VF for filters 1,756 to 34,350 times faster than exhaustive FI. To obtain the vulnerability values for channels, up to 1% of channels are skipped by leveraging the loss function, and up

to 34% of channels require one forward simulation. These results indicate that complete DeepVigor+ provides accurate VF for neurons and channels of CNNs with significantly lower complexity and shorter execution time than exhaustive FI enabled by its optimal fault propagation modeling and analysis.

On the other hand, sampling DeepVigor+ is proposed to further reduce the execution time and complexity of resilience analysis and achieve a scalable method. To show its performance against statistical FI (SFI), Table VI compares the number of simulations for various state-of-the-art SFI [26] with sampling DeepVigor+. As presented, data-aware SFI leads to the least number of executions in FI-based simulation. It is observed that DeepVigor+ sampling activations analysis with 10% channel sampling ratio leads to 8.72 to 20.5 times fewer simulations compared to data-aware SFI. For the filters analysis, DeepVigor+ obtains their VF with 59.4 up to 96.2 times fewer simulations than data-aware SFI.

To obtain the Model Vulnerability Factor (MVF) both activations and filters should be analyzed separately, based on Eq. (15). Therefore, sampling DeepVigor+ accelerates the process from 14.9 up to 26.9 times throughout the DNNs. The scalability and speed of the method are achieved by both channel sampling ratio and logarithmic sampling within them. It can be observed that with the remarkable growth of DNNs under analysis in their number of parameters, the number of simulations in DeepVigor+ does not grow linearly.

To demonstrate the execution time of DeepVigor+ analysis, we employed an A100 NVIDIA GPU and performed sampling DeepVigor+ for activations and filters with different channel sampling ratios. Table VII and Table VIII present the average execution time over 50 executions of the method for complete and sampling DeepVigor+ with different channel sampling ratios, for activations and filters respectively. It is observed

TABLE VI: Comparison of required simulations for statistical FI [26] and sampling DeepVigor+.

Analysis method	Activations Analysis				Filters Analysis			
	Layer-wise	Data-unaware	Data-aware	Sampling DeepVigor+ 10%	Layer-wise	Data-unaware	Data-aware	Sampling DeepVigor+ 10%
VGG-11	74,863	1,562,657	71,173	<b>4,596</b>	75,351	2,141,913	66,934	<b>1,038</b>
VGG-16	117,992	1,839,889	106,513	<b>10,283</b>	123,266	3,588,834	112,151	<b>1,476</b>
ResNet-18-C	188,644	4,264,406	181,911	<b>15,996</b>	189,772	5,253,096	164,159	<b>1,706</b>
MobileNetV2	493,871	8,402,977	452,650	<b>22,077</b>	475,407	8,307,671	259,614	<b>4,364</b>
ResNet-18-I	191,205	5,407,659	189,325	<b>21,680</b>	190,896	5,358,315	167,447	<b>2,178</b>
ResNet-34	344,042	9,624,374	340,383	<b>39,002</b>	344,285	10,031,494	313,484	<b>4,003</b>

that VFs can be obtained in a few minutes for any DNNs. Considering 10% channel sampling ratio for both activations and filters analysis, the total MVF for VGG-11, VGG-16, ResNet-18-C, MobileNet-V2, ResNet-18-I and ResNet-34 is obtained almost in 8.7 minutes, 9.6 minutes, 12.7 minutes, 43.5 minutes, 19.4 minutes and 46 minutes, respectively. It is worth mentioning that the complete DeepVigor+ analysis for the DNNs under study takes almost 22 hours for VGG-16 and 18.5 days for ResNet-34, on the same GPU. Fast execution and accurate estimation of VF obtained by sampling DeepVigor+ analysis provide a remarkable opportunity for a high-speed resilience analysis for any DNN.

TABLE VII: Average execution time over 50 repetitions on A100 GPU for DeepVigor+ activations analysis, with different channel sampling ratios.

DNN	5%	10%	15%	20%	complete analysis
VGG-11	203 sec ( $\approx$ 3.4 min)	415 sec ( $\approx$ 6.9 min)	625 sec ( $\approx$ 10.4 min)	838 sec ( $\approx$ 13.9 min)	66,083 sec ( $\approx$ 0.7 days)
VGG-16	223 sec ( $\approx$ 3.7 min)	453 sec ( $\approx$ 7.5 min)	676 sec ( $\approx$ 11 min)	915 sec ( $\approx$ 15 min)	43,326 sec ( $\approx$ 0.5 days)
ResNet-18-C	284 sec ( $\approx$ 4.7 min)	580 sec ( $\approx$ 9.5 min)	876 sec ( $\approx$ 14.5 min)	1,171 sec ( $\approx$ 19.5 min)	94,939 ( $\approx$ 1.1 days)
MobileNetV2	1,037 sec ( $\approx$ 17 min)	2,097 sec ( $\approx$ 35 min)	3,153 sec ( $\approx$ 52.5 min)	4,071 sec ( $\approx$ 68 min)	211,868 ( $\approx$ 2.4 days)
ResNet-18-I	448 sec ( $\approx$ 7.4 min)	917 sec ( $\approx$ 15 min)	1,390 sec ( $\approx$ 23 min)	1,866 sec ( $\approx$ 31 min)	634,872 ( $\approx$ 7.3 days)
ResNet-34	1,100 sec ( $\approx$ 18 min)	2,237 sec ( $\approx$ 37 min)	3,398 sec ( $\approx$ 56 min)	4,549 sec ( $\approx$ 75 min)	1,402,362 ( $\approx$ 16.2 days)

TABLE VIII: Average execution time over 50 repetitions on A100 GPU for DeepVigor+ filters analysis, with different channel sampling ratios.

DNN	5%	10%	15%	20%	complete analysis
VGG-11	57 sec ( $\approx$ 0.95 min)	111 sec ( $\approx$ 1.8 min)	170 sec ( $\approx$ 2.8 min)	219 sec ( $\approx$ 3.6 min)	23,031 sec ( $\approx$ 0.26 days)
VGG-16	61 sec ( $\approx$ 1 min)	125 sec ( $\approx$ 2.1 min)	168 sec ( $\approx$ 3.1 min)	245 sec ( $\approx$ 4.1 min)	35,634 sec ( $\approx$ 0.4 days)
ResNet-18-C	92 sec ( $\approx$ 1.5 min)	184 sec ( $\approx$ 3 min)	275 sec ( $\approx$ 4.6 min)	367 sec ( $\approx$ 6.1 min)	60,410 sec ( $\approx$ 0.7 days)
MobileNetV2	257 sec ( $\approx$ 4.3 min)	513 sec ( $\approx$ 8.5 min)	759 sec ( $\approx$ 12.6 min)	1,025 sec ( $\approx$ 17.1 min)	39,713 sec ( $\approx$ 0.46 days)
ResNet-18-I	117 sec ( $\approx$ 1.9 min)	250 sec ( $\approx$ 4.1 min)	370 sec ( $\approx$ 6.1 min)	506 sec ( $\approx$ 8.4 min)	134,164 sec ( $\approx$ 1.5 days)
ResNet-34	259 sec ( $\approx$ 4.3 min)	524 sec ( $\approx$ 8.7 min)	795 sec ( $\approx$ 13.2 min)	1,064 sec ( $\approx$ 17.7 min)	201,305 sec ( $\approx$ 2.3 days)

D. Reliability Visualization and Comparison for DNNs

It has been shown that VF for DNNs’ layers and the entire model can be obtained accurately in a few minutes by DeepVigor+. The obtained VF results by DeepVigor+ can be used to visualize the vulnerability of layers within a DNN

and identify more vulnerable ones. Fig. 8 illustrates the LVF comparison for ResNet-18 trained on CIFAR-100 and ImageNet datasets, while total LVF for each layer is obtained based on the numerator of Eq. (15). This visualization sketches how much each layer is vulnerable to single faults compared to each other. As observed, in both ResNet18-C and ResNet18-I first layers are more vulnerable than the latter ones. Therefore, DeepVigor+ enables vulnerability visualization and comparison within a DNN.

Furthermore, DeepVigor+ results in total MVF based on Eq. (15) which is the weighted average of obtained LVFs providing a comprehensive examination of vulnerability between different DNNs. Fig. 9 indicates MVFs for activations and filters of DNNs, separately, as well as their total MVF. As a result, it is observed that activations are more vulnerable than weights. However, weights generally contribute more to the total MVF since their memory footprint is higher than that of activations in DNNs. Based on total MVF, VGG-16 is the least vulnerable DNN (MVF = 1.19%) and MobileNet-V2 is the most vulnerable one (MVF = 2.76%).

E. Impact of Input Data on the Quality of Results

To obtain the VFs in DeepVigor+, we considered one batch of 100 data. Nonetheless, to investigate the impact of data on the quality of analysis results, we repeat the experiments for different batches of data with the size of 100 input data and derive DNNs’ total MVF. Fig. 10 illustrates the obtained total MVF for DNNs over 8 different batches of data. As observed, the variation between the total MVF for each DNN is negligible for different batches of data, demonstrating that analyzing DNNs’ resilience with one batch of data provides confident results.

F. DeepVigor+ Applications and Considerations

As shown, DeepVigor+ achieves a fast, scalable and accurate resilience analysis for emerging DNNs. The analysis provided by DeepVigor+ is not limited to fault resilience assessment, but it can be exploited for designing fault-tolerant and resilient DNNs. Identifying more vulnerable channels and layers can lead to cost-effective selective fault mitigation techniques as well as a comparative investigation between different architectures of DNNs. Moreover, it enables design space exploration to identify more resilient DNNs against faults.

The other output of DeepVigor+ is VVR representing the values that a fault should affect neuron/weight to misclassify DNN’s golden results. These values can be used for obtaining VFs and identifying more vulnerable components as well as for

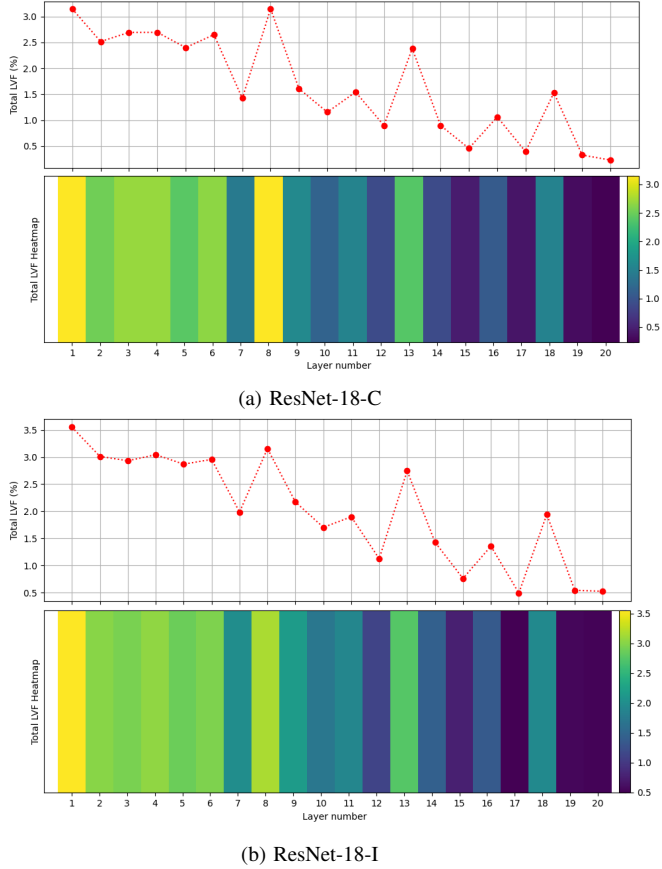


Fig. 8: LVF visualization and comparison for ResNet-18 trained on a) CIFAR-100 and b) ImageNet.

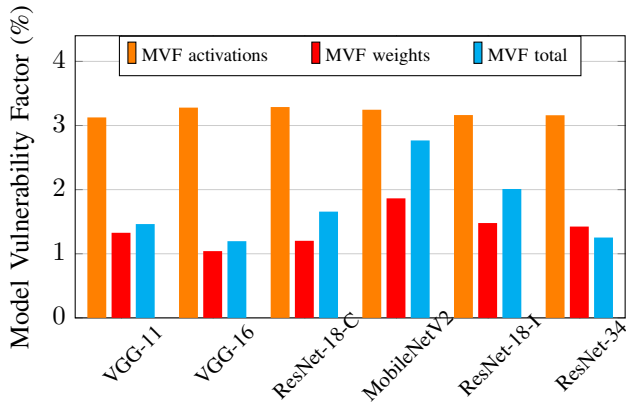


Fig. 9: MVF comparison for DNNs based on activations, filters and the entire model derived by DeepVigor+.

fault detection at inference and identifying bit-level resilience analysis since they are represented in the power of 2 values and can be mapped down to bits.

Yet, there are some constraints in this method to be considered and extended in future research:

- It is assumed that the parameters within the layers of DNNs under analysis are unifiedly distributed among channels and their places are not resorted after training. In such cases, a higher channel sampling ratio is needed

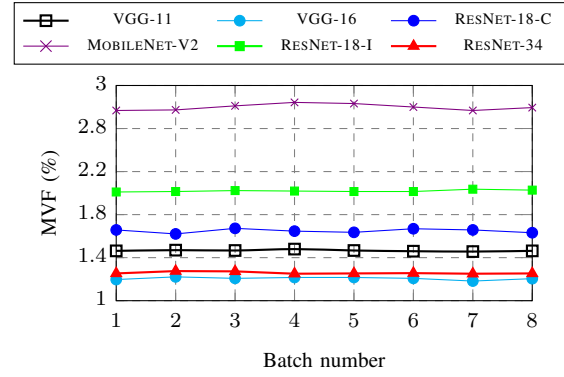


Fig. 10: Total MVF variation over different batches of data for all DNNs.

to obtain accurate VF results.

- DeepVigor+ supports a single-bit fault model in input activations and weights of convolutional layers and obtained VF corresponds to this fault model. For multi-bit fault models, the corresponding error propagation should be applied.
- The error propagation analysis presented in this paper is based on 32-bit floating point data representation. However, the same concept can be extended and applied to fixed-point and integer data representations for QNNs resilience analysis, as in [49].

## VI. CONCLUSION

This paper addresses one of the major challenges in fault resilience analysis for DNNs in the literature. It introduces DeepVigor+, the first semi-analytical scalable alternative method to fault injection, quantifying emerging DNN’s resilience accurately in a short time. DeepVigor+ is facilitated by optimal fault propagation modeling in DNNs accompanied by stratified sampling tackling the scalability problem for resilience analysis for DNNs. This open-source method unleashes a fast resilience assessment, enabling fine-grain evaluation and design space exploration for various fault-tolerant and cost-effective designs for DNNs.

The results in the paper indicate that DeepVigor+ derives vulnerability factors for layers and the entire model of DNNs with less than 1% error, with 14.9 up to 26.9 times fewer simulations than the best-known state-of-the-art statistical FI. It is shown that DNN’s Model Vulnerability Factor can be obtained within minutes by analyzing their activations and weights. DeepVigor+ is presented as an open-source tool for researchers and engineers to enable them to exploit it for DNNs’ fault resilience assessment and enhancement.

## REFERENCES

- [1] Y. Wang and S. H. Chung, “Artificial intelligence in safety-critical systems: a systematic review,” *Industrial Management & Data Systems*, vol. 122, no. 2, pp. 442–470, 2022.
- [2] P. Rech, “Artificial neural networks for space and safety-critical applications: Reliability issues and potential solutions,” *IEEE Transactions on Nuclear Science*, 2024.

- [3] J. Athavale, A. Baldovin, R. Graefe, M. Paulitsch, and R. Rosales, "Ai and reliability trends in safety-critical autonomous systems on ground and air," in *2020 50th Annual IEEE/IFIP International Conference on Dependable Systems and Networks Workshops (DSN-W)*. IEEE, 2020, pp. 74–77.
- [4] I. Moghaddasi, S. Gorgin, and J.-A. Lee, "Dependable dnn accelerator for safety-critical systems: A review on the aging perspective," *IEEE Access*, 2023.
- [5] "Proposal for a regulation of the european parliament and of the council laying down harmonised rules on artificial intelligence (artificial intelligence act) and amending certain union legislative acts," <https://data.consilium.europa.eu/doc/document/ST-5662-2024-INIT/en/pdf>, 2024, [Online].
- [6] "H.r.6216 - national artificial intelligence initiative act of 2020," <https://www.congress.gov/bills/116th-congress/house-bill/6216>, 2020, [Online].
- [7] M. Rausand, *Reliability of safety-critical systems: theory and applications*. John Wiley & Sons, 2014.
- [8] R. Baumann, "The impact of technology scaling on soft error rate performance and limits to the efficacy of error correction," in *Digest. International Electron Devices Meeting*. IEEE, 2002, pp. 329–332.
- [9] J. Henkel, L. Bauer, N. Dutt, P. Gupta, S. Nassif, M. Shafique, M. Tahoori, and N. Wehn, "Reliable on-chip systems in the nano-era: Lessons learnt and future trends," in *Proceedings of the 50th Annual Design Automation Conference*, 2013, pp. 1–10.
- [10] S. Safari, M. Ansari, H. Khdr, P. Gohari-Nazari, S. Yari-Karin, A. Yeganeh-Khaksar, S. Hessabi, A. Ejlali, and J. Henkel, "A survey of fault-tolerance techniques for embedded systems from the perspective of power, energy, and thermal issues," *IEEE Access*, vol. 10, pp. 12 229–12 251, 2022.
- [11] H. Y. Yatbaz, M. Dianati, and R. Woodman, "Introspection of dnn-based perception functions in automated driving systems: State-of-the-art and open research challenges," *IEEE Transactions on Intelligent Transportation Systems*, 2023.
- [12] H. Hussain, P. Tamizharasan, and C. Rahul, "Design possibilities and challenges of dnn models: a review on the perspective of end devices," *Artificial Intelligence Review*, pp. 1–59, 2022.
- [13] R. Desislavov, F. Martínez-Plumed, and J. Hernández-Orallo, "Trends in ai intensive energy consumption: Beyond the performance-vs-parameter laws of deep learning," *Sustainable Computing: Informatics and Systems*, vol. 38, p. 100857, 2023.
- [14] L. Yuan, Y. Chen, T. Wang, W. Yu, Y. Shi, Z.-H. Jiang, F. E. Tay, J. Feng, and S. Yan, "Tokens-to-token vit: Training vision transformers from scratch on imagenet," in *Proceedings of the IEEE/CVF international conference on computer vision*, 2021, pp. 558–567.
- [15] T. Mohaidat and K. Khalil, "A survey on neural network hardware accelerators," *IEEE Transactions on Artificial Intelligence*, 2024.
- [16] Y. Ibrahim, H. Wang, J. Liu, J. Wei, L. Chen, P. Rech, K. Adam, and G. Guo, "Soft errors in dnn accelerators: A comprehensive review," *Microelectronics Reliability*, vol. 115, p. 113969, 2020.
- [17] F. F. Dos Santos, L. Carro, and P. Rech, "Understanding and improving gpus' reliability combining beam experiments with fault simulation," in *2023 IEEE International Test Conference (ITC)*. IEEE, 2023, pp. 176–185.
- [18] T. Garrett, S. Roffe, and A. George, "Soft-error characterization and mitigation strategies for edge tensor processing units in space," *IEEE Transactions on Aerospace and Electronic Systems*, 2024.
- [19] S. Mittal, "A survey on modeling and improving reliability of dnn algorithms and accelerators," *Journal of Systems Architecture*, vol. 104, p. 101689, 2020.
- [20] M. Shafique, M. Naseer, T. Theocharides, C. Kyrkou, O. Mutlu, L. Orosa, and J. Choi, "Robust machine learning systems: Challenges, current trends, perspectives, and the road ahead," *IEEE Design & Test*, vol. 37, no. 2, pp. 30–57, 2020.
- [21] F. Su, C. Liu, and H.-G. Stratigopoulos, "Testability and dependability of ai hardware: Survey, trends, challenges, and perspectives," *IEEE Design & Test*, vol. 40, no. 2, pp. 8–58, 2023.
- [22] M. H. Ahmadilivani, M. Taheri, J. Raik, M. Daneshalab, and M. Jenihhin, "A systematic literature review on hardware reliability assessment methods for deep neural networks," *ACM Computing Surveys*, vol. 56, no. 6, pp. 1–39, 2024.
- [23] —, "Deepvigor: Vulnerability value ranges and factors for dnn reliability assessment," in *2023 IEEE European Test Symposium (ETS)*. IEEE, 2023, pp. 1–6.
- [24] A. Canziani, A. Paszke, and E. Culurciello, "An analysis of deep neural network models for practical applications," *arXiv preprint arXiv:1605.07678*, 2016.
- [25] Z. Chen, G. Li, K. Pattabiraman, and N. DeBardeleben, "Binfi: An efficient fault injector for safety-critical machine learning systems," in *Proceedings of the International Conference for High Performance Computing, Networking, Storage and Analysis*, 2019, pp. 1–23.
- [26] A. Ruospo, G. Gavarini, C. De Sio, J. Guerrero, L. Sterpone, M. S. Reorda, E. Sanchez, R. Mariani, J. Aribido, and J. Athavale, "Assessing convolutional neural networks reliability through statistical fault injections," in *2023 Design, Automation & Test in Europe Conference & Exhibition (DATE)*. IEEE, 2023, pp. 1–6.
- [27] A. Mahmoud, N. Aggarwal, A. Nobe, J. R. S. Vicarte, S. V. Adve, C. W. Fletcher, I. Frosio, and S. K. S. Hari, "Pytorchfi: A runtime perturbation tool for dnn," in *2020 50th Annual IEEE/IFIP International Conference on Dependable Systems and Networks Workshops (DSN-W)*, 2020, pp. 25–31.
- [28] O. Weng, A. Meza, Q. Bock, B. Hawks, J. Campos, N. Tran, J. M. Duarte, and R. Kastner, "Fkeras: A sensitivity analysis tool for edge neural networks," *Journal on Autonomous Transportation Systems*, 2024.
- [29] N. Khoshavi, C. Broyles, Y. Bi, and A. Roohi, "Fiji-fin: A fault injection framework on quantized neural network inference accelerator," in *2020 19th IEEE International Conference on Machine Learning and Applications (ICMLA)*. IEEE, 2020, pp. 1139–1144.
- [30] M. Taheri, M. H. Ahmadilivani, M. Jenihhin, M. Daneshalab, and J. Raik, "Appraiser: Dnn fault resilience analysis employing approximation errors," in *2023 26th International Symposium on Design and Diagnostics of Electronic Circuits and Systems (DDECS)*. IEEE, 2023, pp. 124–127.
- [31] M. Taheri, M. Daneshalab, J. Raik, M. Jenihhin, S. Pappalardo, P. Jimenez, B. Deveautour, and A. Bosio, "Saffira: a framework for assessing the reliability of systolic-array-based dnn accelerators," in *2024 27th International Symposium on Design & Diagnostics of Electronic Circuits & Systems (DDECS)*. IEEE, 2024, pp. 19–24.
- [32] Z. Chen, N. Narayanan, B. Fang, G. Li, K. Pattabiraman, and N. DeBardeleben, "Tensorfi: A flexible fault injection framework for tensorflow applications," in *2020 IEEE 31st International Symposium on Software Reliability Engineering (ISSRE)*. IEEE, 2020, pp. 426–435.
- [33] S. Laskar, M. H. Rahman, and G. Li, "Tensorfi+: a scalable fault injection framework for modern deep learning neural networks," in *2022 IEEE International Symposium on Software Reliability Engineering Workshops (ISSREW)*. IEEE, 2022, pp. 246–251.
- [34] R. Leveugle, A. Calvez, P. Maistri, and P. Vanhauwaert, "Statistical fault injection: Quantified error and confidence," in *2009 Design, Automation & Test in Europe Conference & Exhibition*. IEEE, 2009, pp. 502–506.
- [35] C. Schorn, A. Guntero, and G. Ascheid, "Accurate neuron resilience prediction for a flexible reliability management in neural network accelerators," in *2018 Design, Automation & Test in Europe Conference & Exhibition (DATE)*. IEEE, 2018, pp. 979–984.
- [36] J. Wang, J. Zhu, X. Fu, D. Zang, K. Li, and W. Zhang, "Enhancing neural network reliability: Insights from hardware/software collaboration with neuron vulnerability quantization," *IEEE Transactions on Computers*, 2024.
- [37] C. Amarnath, M. Mejri, K. Ma, and A. Chatterjee, "Soft error resilient deep learning systems using neuron gradient statistics," in *2022 IEEE 28th International Symposium on On-Line Testing and Robust System Design (IOLTS)*. IEEE, 2022, pp. 1–7.
- [38] —, "Error resilience in deep neural networks using neuron gradient statistics," *IEEE Transactions on Computer-Aided Design of Integrated Circuits and Systems*, 2023.
- [39] M. Sabih, F. Hannig, and J. Teich, "Fault-tolerant low-precision dnn using explainable ai," in *2021 51st Annual IEEE/IFIP International Conference on Dependable Systems and Networks Workshops (DSN-W)*. IEEE, 2021, pp. 166–174.
- [40] A. Mahmoud, S. K. S. Hari, C. W. Fletcher, S. V. Adve, C. Sakr, N. Shanbhag, P. Molchanov, M. B. Sullivan, T. Tsai, and S. W. Keckler, "Hardnn: Feature map vulnerability evaluation in cnns," *arXiv preprint arXiv:2002.09786*, 2020.
- [41] I. Chatterjee, B. Narasimham, N. Mahatme, B. Bhuvra, R. Reed, R. Schrimpf, J. Wang, N. Vedula, B. Bartz, and C. Monzel, "Impact of technology scaling on sram soft error rates," *IEEE Transactions on Nuclear Science*, vol. 61, no. 6, pp. 3512–3518, 2014.
- [42] M. B. Sullivan, N. Saxena, M. O'Connor, D. Lee, P. Racunas, S. Hukerikar, T. Tsai, S. K. S. Hari, and S. W. Keckler, "Characterizing and mitigating soft errors in gpu dram," in *MICRO-54: 54th Annual IEEE/ACM International Symposium on Microarchitecture*, 2021, pp. 641–653.
- [43] Z. Yan, Y. Shi, W. Liao, M. Hashimoto, X. Zhou, and C. Zhuo, "When single event upset meets deep neural networks: Observations, explorations, and remedies," in *2020 25th Asia and South Pacific Design Automation Conference (ASP-DAC)*. IEEE, 2020, pp. 163–168.

- [44] M. Bushnell and V. Agrawal, *Essentials of electronic testing for digital, memory and mixed-signal VLSI circuits*. Springer Science & Business Media, 2004, vol. 17.
- [45] J. Elliott, F. Mueller, F. Stoyanov, and C. Webster, “Quantifying the impact of single bit flips on floating point arithmetic,” North Carolina State University, Dept. of Computer Science, Tech. Rep., 2013.
- [46] J. Zhan, R. Sun, W. Jiang, Y. Jiang, X. Yin, and C. Zhuo, “Improving fault tolerance for reliable dnn using boundary-aware activation,” *IEEE Transactions on Computer-Aided Design of Integrated Circuits and Systems*, vol. 41, no. 10, pp. 3414–3425, 2021.
- [47] Z. Huang, W. Shao, X. Wang, L. Lin, and P. Luo, “Rethinking the pruning criteria for convolutional neural network,” *Advances in Neural Information Processing Systems*, vol. 34, pp. 16 305–16 318, 2021.
- [48] R. Singh, N. S. Mangat, R. Singh, and N. S. Mangat, “Stratified sampling,” *Elements of survey sampling*, pp. 102–144, 1996.
- [49] M. H. Ahmadilivani, M. Taheri, J. Raik, M. Daneshtalab, and M. Jenihhin, “Enhancing fault resilience of qnns by selective neuron splitting,” in *2023 IEEE 5th International Conference on Artificial Intelligence Circuits and Systems (AICAS)*. IEEE, 2023, pp. 1–5.



**Mohammad Hasan Ahmadilivani** is a PhD student in the Computer Systems Department at Tallinn University of Technology (Taltech), Estonia. He earned his MSc in Computer Architecture Systems from the University of Tehran, Iran, in 2020. His research focuses on developing analytical methods to measure and enhance the hardware reliability of deep neural networks (DNNs). His research interests include exploiting DNNs in safety-critical applications, robust computer vision, and efficient and reliable DNN accelerator design.



**Jaan Raik** is a Full Professor at the Department of Computer Systems and Head of the Center for Dependable Computing Systems at the Tallinn University of Technology (Taltech), Estonia. He received his M.Sc. and Ph.D. degrees from Taltech in 1997 and in 2001, respectively. His research interests cover a wide area in electrical engineering and computer science domains including reliability of deep learning, hardware test, functional verification, fault-tolerance and security as well as emerging computer architectures. He has co-authored more than 400 scientific publications. He is a member of IEEE Computer Society, HiPEAC and of Steering/Program Committees of numerous conferences within his field. He served as the General Chair to IEEE European Test Symposium '25, '20, IFIP/IEEE VLSI-SoC '16, DDECS '12), Vice General Chair IEEE European Test Symposium '24, DDECS '13 and Program Co-Chair DDECS '23, '15, CDN-Live '16 conferences. He was awarded the Global Digital Governance Fellowship at Stanford (2022) and HiPEAC Paper Award (2020).



**Masoud Daneshtalab** Masoud Daneshtalab is currently a full Prof. at Mälardalen University in Sweden, Adj. Prof. at TalTech in Estonia and leads the Heterogeneous System research group. He is on the Euromicro board of directors, an editor of the MICPRO journal, and has published over 200 refereed papers. His research interests include HW/SW/Algorithm co-design, dependability and deep learning acceleration.



**Maksim Jenihhin** is a tenured associate professor of computing systems reliability and Head of the research group Trustworthy and Efficient Computing Hardware (TECH) at the Tallinn University of Technology, Estonia. He received his PhD degree in Computer Engineering from the same university in 2008. His research interests include reliable and efficient hardware for AI acceleration, methodologies and EDA tools for hardware design, verification and security, as well as nanoelectronics reliability and manufacturing test topics. He has published more than 170 research papers, supervised several PhD students and postdocs and served on executive and program committees for numerous IEEE conferences (DATE, ETS, DDECS, LATS, NORCAS, etc.). Prof. Jenihhin coordinates European collaborative research projects HORIZON MSCA DN “TIRAMISU” (2024), HORIZON TWINN “TAICHIP” (2024) and national ones about energy efficiency and reliability of edge-AI chips and cross-layer self-health awareness of autonomous systems.